Multiyear riparian evapotranspiration and groundwater use for a semiarid watershed

R.L. Scott[a],*, W.L. Cable[a], T.E. Huxman[b], P.L. Nagler[c],
M. Hernandez[a], D.C. Goodrich[a]

[a]*Southwest Watershed Research Center, USDA-ARS, 2000 E. Allen Road, Tucson, AZ 85719, USA*
[b]*Department of Ecology and Evolutionary Biology, University of Arizona, Tucson, AZ 85721, USA*
[c]*US Geological Survey, Southwest Biological Science Center, Sonoran Desert Research Station, University of Arizona, Tucson, AZ 85721, USA*

Abstract

Riparian evapotranspiration (ET) is a major component of the surface and subsurface water balance for many semiarid watersheds. Measurement or model-based estimates of ET are often made on a local scale, but spatially distributed estimates are needed to determine ET over catchments. In this paper, we document the ET that was quantified over 3 years using eddy covariance for three riparian ecosystems along the Upper San Pedro River of southeastern Arizona, USA, and we use a water balance equation to determine annual groundwater use. Riparian evapotranspiration and groundwater use for the watershed were then determined by using a calibrated, empirical model that uses 16-day, 250–1000 m remote-sensing products for the years of 2001–2005. The inputs for the model were derived entirely from the NASA MODIS sensor and consisted of the Enhanced Vegetation Index and land surface temperature. The scaling model was validated using subsets of the entire dataset (omitting different sites or years) and its capable performance for well-watered sites ($MAD = 0.32\,mm\,day^{-1}$, $R^2 = 0.93$) gave us confidence in using it to determine ET over the watershed. Three years of eddy covariance data for the riparian sites reveal that ET and groundwater use increased as woody plant density increased. Groundwater use was less variable at the woodland site, which had the greatest density of phreatophytes. Annual riparian groundwater use within the watershed was nearly constant over the study period despite an on-going drought. For the San Pedro alone, the amounts determined in this paper are within the range of most recently reported values that were derived using an entirely different approach. However, because of our larger estimates for groundwater use for the main tributary of the San Pedro, the watershed totals were higher. The approach presented here can provide riparian ET and groundwater use amounts that reflect real natural variability in phreatophyte withdrawals and improve the accuracy of a watershed's water budget.

© 2008 Elsevier Ltd. All rights reserved.

Keywords: Eddy covariance; Evapotranspiration; MODIS; Remote sensing; Riparian water use

*Corresponding author. Tel.: +1 520 670 6380x113; fax: +1 520 670 5550.
  E-mail address: russ.scott@ars.usda.gov (R.L. Scott).

1. Introduction

For many arid and semiarid watersheds, riparian evapotranspiration (ET) is a major part of the surface and subsurface water balance. Riparian ET can be derived from surface water sources like recently fallen precipitation in the streams and vadose zone and from groundwater sources acquired by phreatophytic plants or directly evaporated from base flow in the river. Accurate estimates of ET at watershed and basin scales are necessary for sound water resource management, especially in basins where there is limited water to support human communities and natural riparian ecosystems (e.g., Devitt et al., 2002; Lines and Bilhorn, 1996; Scott et al., 2000; Steinwand et al., 2006; Westenburg et al., 2006). Over the last decade, many studies in the western US have advanced the understanding of riparian ET by making direct micrometeorological and physiological ET measurements for different riparian cover types (Cleverly et al., 2002; Dahm et al., 2002; Devitt et al., 1998; Gazal et al., 2006; Schaeffer et al., 2000; Scott et al., 2000, 2004, 2006a; Unland et al., 1998). Some attempts have been made to scale these measurements up to catchments or river reaches, but the understanding of how ET varies from year-to-year and from site-to-site has been limited (Goodrich et al., 2000; Scott et al., 2006b; Westenburg et al., 2006).

Essentially, two basic approaches have been used to produce river-reach-scale estimates of riparian ET from site measurements. The first is to quantify ET by making measurements at sites that are representative of major riparian assemblages and then determine ET over a river reach of interest by multiplying the total area of the different cover types by their respective ET rates (e.g., Dahm et al., 2002; Goodrich et al., 2000; Scott et al., 2006b; Westenburg et al., 2006). Because of the limited field measurements available, this approach is necessary to obtain reach-scale estimates but unfortunately does not account for the spatial variability in ET along the riparian corridor. Because a few measurements might not accurately be representative across the area of interest, the second approach involves using a model, typically employing spatially distributed
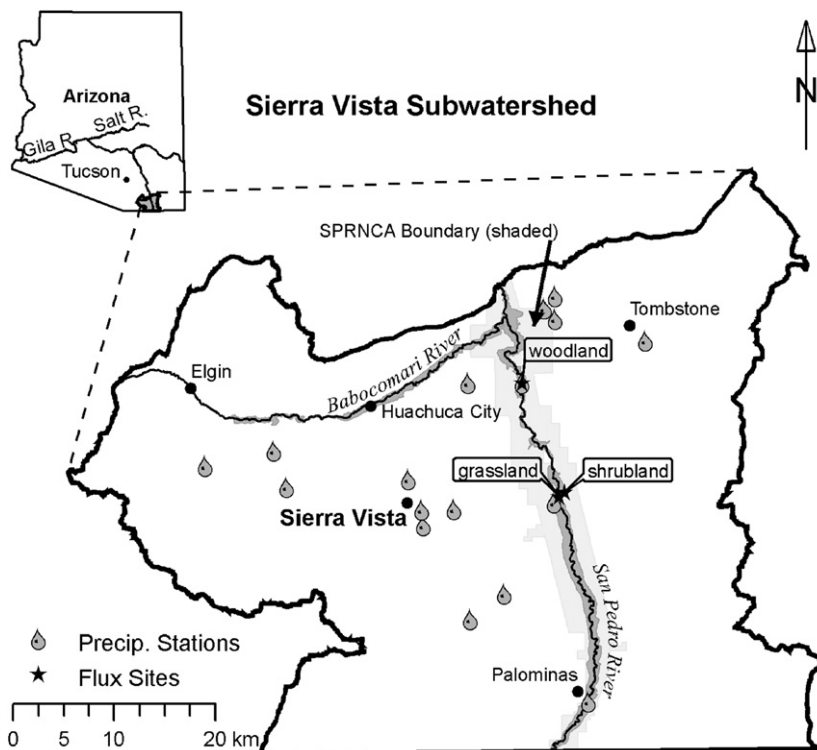
Fig. 1. The Sierra Vista Subwatershed of the Upper San Pedro River Basin, Arizona, USA. The location of the three riparian flux sites and the 17 rain gages used to determine annual rainfall over the riparian corridor are shown. The boundary of the San Pedro Riparian National Conservation Area (SPRNCA) and the narrow riparian corridor along the San Pedro and Babocomari rivers over which evapotranspiration and groundwater use were determined are also highlighted.

remotely sensed products, to simulate ET. This has become more feasible as regular overpasses and finer-resolution satellite data have become available. One modeling strategy has been to estimate components of surface energy balance by using a combination of ground and remote-sensing measurements (e.g., Bastiaanssen et al., 2002; Loheide and Gorelick, 2005). Recently, a combined approach has been used that extends empirical relationships between satellite-derived vegetation indices and tower-based ET measurements to a river of interest (Nagler et al., 2005a, b).

The objective of this work was to report on measurements of ET from three sites and to produce multiyear estimates of riparian ET and groundwater use (ET_{gw}) at a spatial scale useful for water resource management. The study basin was the Sierra Vista Subwatershed of the Upper San Pedro River Basin in southeastern Arizona (Fig. 1). Riparian ET, and in particular ET_{gw}, have received substantial attention in this basin due to the concern about the long-term effects of groundwater pumping on the integrity of the riparian corridor's streamflow and habitat (Steinitz et al., 2003). We monitored ET using the eddy covariance technique over a floodplain grassland, shrubland, and woodland from 2003 through 2005. We used these measurements to develop an empirical relationship between ET and remotely sensed data in order to up-scale ET and ET_{gw} for the two main river reaches within the catchment for 2001–2005. Because previous attempts to quantify riparian ET in this basin have used mainly 1-year ET datasets and a static vegetation map for up-scaling (Goodrich et al., 2000; Scott et al., 2006b), this approach represents a significant update, with novel features that account for climate and vegetation variability in an expanded multiyear framework.

2. Background on determining riparian ET in the San Pedro Basin

In 1988, Congress designated portions of the San Pedro River in the Upper San Pedro Basin in Arizona as the San Pedro Riparian National Conservation Area (SPRNCA). This conservation area protects a river with portions of perennial and intermittent flow and an ecologically diverse and important riparian habitat (Kingsolver, 2000). The basin also hosts growing populations of residents in areas hydraulically up-gradient from sensitive reaches of the riparian system. The largest amount of pumping in the basin and most of the perennial portions of the San Pedro River are located within a part of the basin called the Sierra Vista Subwatershed (Fig. 1). Residents of several local communities within this subwatershed have responded to the need for water planning by forming the Upper San Pedro Partnership (USPP), a consortium of 21 agencies and organizations with a primary goal of ensuring long-term water needs for both the area residents and for the riparian vegetation and wildlife within the SPRNCA (Browning-Aiken et al., 2004; http://www.usppartnership.com).

As part of the overall planning strategy, the USPP tasked a multidisciplinary team of researchers to better characterize the hydrology of the Upper San Pedro Basin including that of the SPRNCA (Leenhouts et al., 2006). One facet of this work has been to quantify the riparian ET in the Upper San Pedro Basin (Scott et al., 2006b). Scott et al. (2006b) used a host of different measurement strategies made for different ecosystems and dominant plant types within the SPRNCA to estimate riparian groundwater use for 2003, the year in which measurements were available from all the sites of their study. Their approach was to make micrometeorological and plant physiological measurements of riparian ET of major riparian assemblages, and then use a combination of isotope and water balance techniques to partition that ET into ET_{gw}. Finally, to scale up over different river reaches of interest, they multiplied the total area of the different cover types from a detailed vegetation map by their respective groundwater use rates.

The work of Scott et al. (2006b) represents an expansion of the work by Goodrich et al. (2000) who were the first to use direct measurements to determine riparian ET and groundwater use along the San Pedro. Prior to Goodrich et al. (2000), Corell et al. (1996) estimated riparian groundwater use by exploiting the difference between river base flows in winter and summer at the USGS surface water gauges in the basin. Using entirely different approaches, both estimates are surprisingly similar (Table 1), but considerably lower than those of Scott et al. (2006b). The range of water use given by Scott et al. (2006b) is due to the uncertainty of quantifying the amount of riparian vegetation from the most recent vegetation map, which listed ranges rather than exact percentages of vegetation cover for certain types of vegetation polygons.

Table 1
Previous annual riparian groundwater use estimates for the San Pedro River within the Sierra Vista Subwatershed

Corell et al. (1996)[a]	$8758 \times 10^3\,\text{m}^3$
Goodrich et al. (2000)[b]	$8130 \times 10^3\,\text{m}^3$
Scott et al. (2006b)[b]	$9065–11,112 \times 10^3\,\text{m}^3$

[a]From the start of the perennial reach upstream of the USGS Palominas gauge to the USGS Tombstone gauge.
[b]From the international border to the USGS Tombstone gauge.

3. Methods

3.1. Measurements

ET data were collected using the eddy covariance technique from micrometeorological towers located over: (1) a mesquite (*Prosopis velutina*) woodland, (2) a sacaton (*Sporobolus wrightii*) grassland, and (3) a mixed mesquite/sacaton shrubland along the main stem of the San Pedro River. Measurements used in this study spanned the years 2003–2005. Scott et al. (2004) describe the woodland site in detail and document the water and carbon dioxide fluxes measured in 2001 and 2002. Scott et al. (2006a) compared all three sites for water and carbon dioxide measurements made in 2003. This study includes these previously reported measurements plus an additional 2 years of data from each of these sites collected in 2004 and 2005. Scott et al. (2004, 2006a) give details about the eddy covariance instrumentation and methods along with site descriptions.

Studies incorporating eddy covariance instrumentation commonly use the standard of energy balance closure to evaluate the accuracy and efficacy of their measurements (Wilson et al., 2002). The average daily closure ratio ($[\lambda E+H]/[R_n-G]$) for the sites used in this study ranged annually from 0.89 to 0.92 for the woodland, 0.81 to 0.83 for the shrubland, and 0.76 to 0.78 for the grassland. While not ideal, these values are consistent with numerous other studies (Wilson et al., 2002).

One of the goals of this study was to quantify the magnitude and variability of the seasonal water use of the riparian vegetation. It was necessary to recognize the shortcomings in closure when doing this, especially since the degree of closure was different between the years that we compared. For our analysis we chose to follow Twine et al. (2000) who suggested that forcing closure was justified when available energy was known and errors in its measurement modest. Consequently, we scaled our latent and sensible heat fluxes to force daily closure while conserving the measured Bowen ratio. Closing the daily energy balance, rather than the half-hour balance, was preferred because energy storage between the land surface and the eddy covariance sensors was unmeasured and likely significant over 30 min, but not at a daily time-scale.

In the following analysis, daily average ET values were calculated by first filling the gaps in the 30-min data that were due to sensor malfunctions or bad measurements. Gaps were filled using 30-min averages of photosynthetic photon flux density (ppfd) and 14-day look-up tables of ET values averaged over $100\,\mu\text{moles}\,\text{m}^{-2}\,\text{s}^{-1}$ intervals (Falge et al., 2001). Occasional multiday periods with no available data, including ppfd, were filled by interpolating across the period using the data from 3 days prior to and following the data gap. For the calibration and verification of the empirical scaling relationship, gap-filled, daily ET were used to compute 16-day averages that were in sync with the 16-day satellite data.

In order to compare the results of this study with a reference evaporation rate that can be computed with standard meteorological data alone, we computed the reference crop evaporation rate, E_{rc} (Shuttleworth, 1993). The reference crop evaporation is an estimate of the evaporation, which would occur from a short, well-watered grass with a fixed-height of 0.12 m, an albedo of 0.23 and a surface resistance of $69\,\text{s}\,\text{m}^{-1}$. It is calculated in units of $\text{mm}\,\text{day}^{-1}$ by the following formula:

$$E_{\text{rc}} = \frac{\Delta(R_{\text{net}} - G)}{\Delta + \gamma^*} + \frac{\gamma}{\Delta + \gamma^*}\frac{900}{(T + 275)}U_2 D,$$

where R_{net} is the net radiation exchange for the crop cover ($\text{mm}\,\text{day}^{-1}$), G is the soil heat flux ($\text{mm}\,\text{day}^{-1}$), T is the air temperature (°C), U_2 is the wind speed at 2 m ($\text{m}\,\text{s}^{-1}$), D is the vapor pressure deficit (kPa), Δ is the slope of the saturation vapor pressure versus temperature curve, γ is the psychrometric constant ($\text{kPa}\,°\text{C}^{-1}$),

and γ^* is a modified psychrometric constant (kPa $°C^{-1}$). The evaporation rate from a well-watered crop or vegetation community can differ from that of a reference crop of well-watered grass. Typical differences are $\pm$10–20% (Shuttleworth, 1993).

In order to understand possible controls on evaporation, we also monitored the state of the vadose zone soil moisture and the depth to groundwater. Soil thermocouples and water content reflectometers (CS-616; Campbell Scientific Inc., Logan, UT) were installed in a vertical profile at 0.05, 0.1, 0.25, 0.5, 0.7, and 1.0 m depth to measure the soil moisture every 30 min under the each site. A piezometer was installed and equipped with a water level monitor (miniTROLL, In-Situ Inc., Ft. Collins, CO) at each site to measure the fluctuations in the water table every 30 min.

3.2. Determination of annual groundwater use

To determine the annual site- and reach-scale groundwater use, we used the water balance equation:

$$\text{ET}_{gw} = \text{ET} - (P - \Delta S), \tag{1}$$

where ET_{gw} is groundwater use, ET is total evapotranspiration, P is precipitation, and ΔS is the change of soil moisture in the top 1 m of soil. At the three instrumented sites, we assumed that runoff was negligible due to the locally flat topography, and that there were only small changes in soil moisture deeper than 1 m as suggested by measured soil moisture profiles at each site. Thus ET_{gw}, if positive, is the ET in excess of precipitation and change in near-surface soil moisture storage. We assumed that all of the excess moisture was derived from groundwater.

To obtain reach-scale groundwater use, ET was modeled every 16 days and then summed to compute an annual total for each 250 m riparian pixel (Section 3.3). Annual 2001–2005 precipitation for each pixel was determined by using the inverse-distance-square weighting method (Smith, 1993) and the rainfall totals from 17 rain gauges in the watershed (Fig. 1). While unknown, we assumed annual soil moisture storage changes (ΔS) to be small, and therefore, set them to be zero. Likewise, runoff or run-on from each pixel was assumed to be zero. For most pixels along the riparian bottomland, this was a fair assumption though there were undoubtedly some pixels that had considerable runoff or run-on. We assumed that these cases averaged out to zero when calculating groundwater use over the reach scale.

3.3. ET scaling

For scaling ET measurements up to compute reach total water use, we developed an empirical relationship between ET and MODIS Enhanced Vegetation Index (EVI; Huete et al., 2002) and land surface temperature (T_s) following an approach similar to Nagler et al. (2005a, b). To do this, we used the equation:

$$\text{ET} = a(1 - e^{-b\text{EVI}}) + c\,e^{dT_s} + e, \tag{2}$$

where a, b, c, d, and e are regression parameters. In Eq. (2), EVI, T_s, were acquired entirely from MODIS products and did not require any ground data. EVI was the composite 16-day, 250 m product (MOD13Q1). T_s was obtained from the nighttime land surface temperature (8-day composite, 1 km, MOD11A2). Before fitting Eq. (2), all of the data were first averaged up temporally to meet the resolution of the 16-day MODIS data and T_s was interpolated spatially onto the 250 m EVI pixel.

Eq. (2) is similar to the approach of Nagler et al. (2005b), but the form of the equation was changed as it produced improved calibration results and reduced the number of parameters from 6 to 5. Also, we did not find it necessary to scale EVI, and we used a MODIS-derived estimate of nighttime surface temperature instead of a locally measured air temperature. We found a high degree of correlation between T_s and air temperature for all sites ($R^2 = 0.95$), and nighttime temperatures produced better model fits than daytime ones.

The regression parameters in Eq. (2) were determined in two steps. First, the Shuffled Complex Evolution Metropolis (SCEM-UA) algorithm (Vrugt et al., 2003) was used to estimate the most likely parameter set and its underlying posterior probability distribution within a single optimization run. This algorithm is related to the successful SCE-UA global optimization algorithm and merges the strengths of the Metropolis Hastings

algorithm, controlled random search, competitive evolution and complex shuffling in order to evolve to a stationary posterior target distribution of the parameters. After generating the posterior distribution for each parameter, the sample quartiles $q_{0.25}$, $q_{0.50}$, and $q_{0.75}$ were computed and used in the second step of the parameter estimation process. In order to evaluate the uncertainty in the estimation of the coefficients in Eq. (2), the error matrix was computed. Then, a simple gradient-search method was used to estimate the optimal parameter set. From the analysis carried out in the first step, the quartile $q_{0.50}$ values were used as initial starting estimates of the parameters. The gradient-search method requires upper and lower limits of the parameters, the lower limit was set for each parameter based on the $q_{0.25}$ and the upper limit was based on the $q_{0.75}$ values. The gradient-search method was set to find the optimal parameter set that minimizes the mean absolute difference (MAD) function defined as

$$\text{MAD} = \frac{\sum_{i=1}^{n} |\text{ET}(i)_{\text{obs}} - \text{ET}(i)_{\text{sim}}|}{n}, \tag{3}$$

where $\text{ET}(i)_{\text{obs}}$ is the observed ET at time (i) and $\text{ET}(i)_{\text{sim}}$ is estimated ET at time (i). The parameter estimation analysis yielded the optimal parameter set, its confidence intervals, and the covariance matrix of the estimated parameters.

In order to estimate the uncertainty in the calculated value of ET, which results from the uncertainty in the parameters and independent variables (EVI and T_s), we used the Gaussian error propagation method (Bevington and Robinson, 1992). The Gaussian error propagation equation is described by

$$\sigma_{\text{et}}^2 = \sum_{i=1}^{n} \sigma_{xi}^2 \left(\frac{\partial \text{et}}{\partial xi}\right)^2 + 2\sum_{i=1}^{n}\sum_{j=1}^{n} \sigma_{xi,xj}^2 \left(\frac{\partial \text{et}}{\partial xi}\right)\left(\frac{\partial \text{et}}{\partial xj}\right), \quad i \neq j, \tag{4}$$

where x_1, x_2, …, x_n represent the n input variables and coefficients, and σ_{x1}, σ_{x2}, …, σ_{xn} are their associated errors (i.e., standard deviations). ET is a function of the input variables and regression coefficients, and the error in ET is denoted by σ_{et}. The estimated errors (σ) for the model input varied in the literature so we used estimates that were in the middle of the range we found: 0.05 for EVI and 0.5 °C for T_s.

4. Results

4.1. Hydrologic conditions and ET

Throughout most of the 2001–2005 study period, southeastern Arizona was under drought conditions. Accordingly, seasonal precipitation totals at the riparian sites were usually below average (Fig. 2). Wetter-than-average or near-normal precipitation fell at most of the sites only during the pre-monsoon (March–June) of 2001 and 2004 and the monsoon period (July–October) of 2005. Drier-than-average conditions were especially evident in winter (November–February) and pre-monsoon periods of 2002 and 2003. The winter and pre-monsoon periods of 2001 had anomalously high soil moisture conditions (Fig. 3) due to a large amount of precipitation (125–254 mm) that fell in the basin in October 2000.

Since extended periods of no rainfall and high evaporation demand are common in dryland regions, it is difficult to discern the effects of meteorological drought conditions on soil moisture because soil moisture levels are essentially "reset" to near-zero levels during these protracted periods every year. There was a very slight decreasing trend in lower root zone soil moisture at the woodland (Fig. 3). However, most of the soil moisture variation was within the upper 0.3 m of the surface, and the soil moisture dynamics generally followed a similar pattern from year-to-year at all depths. Soil moisture at 1 m was usually highest during the winter and lowest before the monsoon onset. At the woodland, upper root zone (0–0.3 m) moisture peaked during winter 2001, the wet monsoon of 2002 and in the winter of 2004. Similar variations in soil moisture occurred at the other two riparian flux sites during the 2003–2005 period when they were monitored (data not shown).

Despite the on-going 2001–2005 drought conditions, there were no major trends in groundwater depths (Fig. 4). On an annual basis, water levels rose throughout the winter then declined rapidly following the leafing out of the riparian vegetation and subsequent onset of phreatophyte transpiration. Prior to the start of
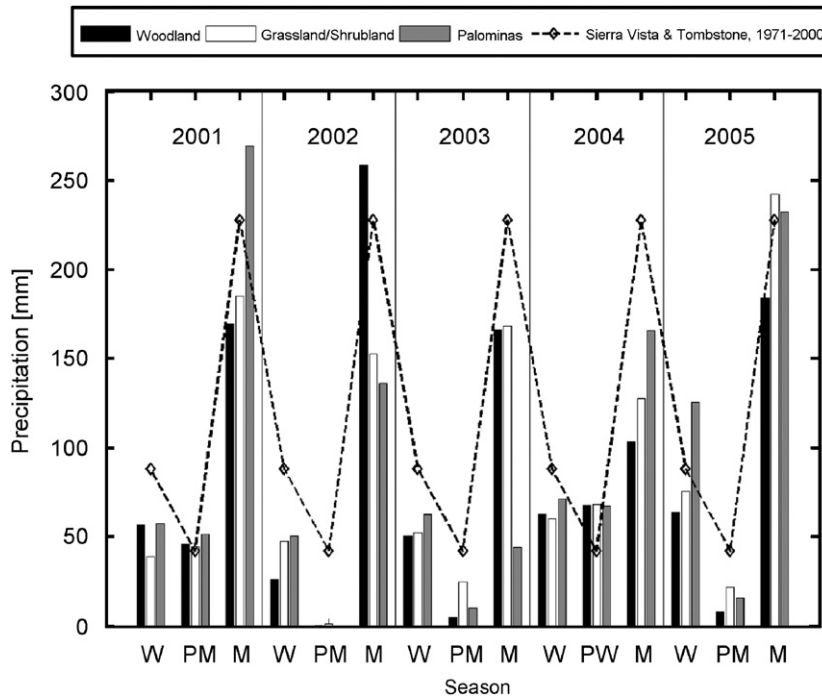
Fig. 2. 2001–2005 total winter (W = November–February), pre-monsoon (PM = March–June), and monsoon (M = July–October) precipitation for three riparian met sites. The means of the 1971–2000 Sierra Vista and Tombstone, AZ climate normals are also shown.
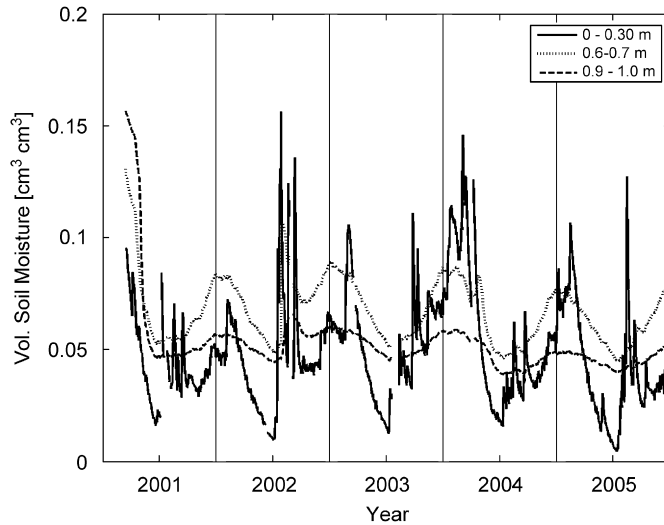
Fig. 3. Daily average soil moisture for shallow (0–0.3 m) and deeper (> 0.6 m) depths at the woodland site.

summer precipitation, water levels reached their lowest elevation but then rebounded with the arrival of monsoon rains and flood flows in the nearby river, which readily recharged the floodplain aquifer. In fall, water levels eventually rose again as declining light levels and temperatures reduced, and eventually halted, phreatophyte transpiration The wells at the proximate grassland and shrubland sites were located along a perennial flow reach of the river that generally buffered annual fluctuations in depth to groundwater (Fig. 4b–c). The pre-monsoon drawdowns were greater and the water table had a slight decreasing trend at the
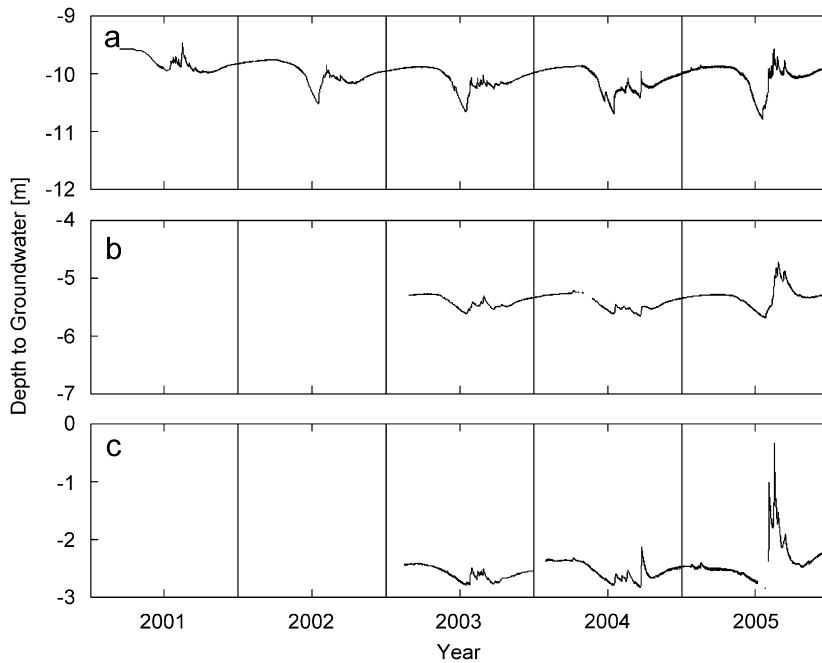
Fig. 4. Depth to groundwater for the three riparian flux sites.
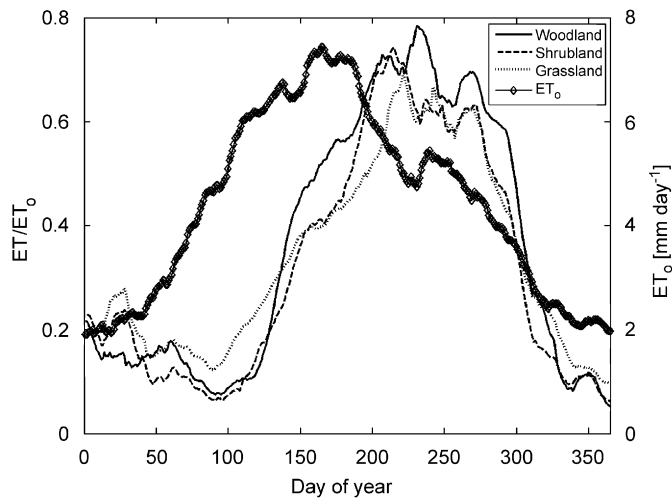
Fig. 5. 2003–2005 average reference crop factor (ET/ET_o) for each site and average reference crop evaporation (ET_o) from all sites.

woodland, which was located along a losing or intermittent flow reach (Fig. 4a). The water table elevations at all sites reached their lowest level in July 2005 in part due to the second latest start to the monsoon on record.

Both riparian vegetation phenology and rainfall had a major influence on determining the seasonal magnitude of ET/ET_o (Fig. 5). The grassland was the first to leaf out in spring as the mesquite trees at the other two sites were more frost intolerant. During the early part of the growing season when ET_o was highest, ET/ET_o was nearly equivalent at the shrubland and grassland and highest for woodland. During the monsoon ET_o was depressed due to the decrease in radiation (cloudy days) and lower VPD, while ET/ET_o peaked at all sites. As the monsoon rains tapered off, ET_o rebounded slightly while ET/ET_o remained high for several more weeks before rapidly decreasing with the arrival of the winter.

Table 2
Annual site water balance components (Eq. (1))

	2003			2004			2005		
	Woodland	Shrubland[a]	Grassland[b]	Woodland	Shrubland	Grassland	Woodland	Shrubland	Grassland
ET	746	591	581	721	687	634	713	704	715
P	232	252	252	227	261	261	236	312	312
ΔS	2	0	0	−18	−4	−4	−2	−11	0
$P-\Delta S$	230	252	252	244	266	265	238	324	312
ET_{gw}	517	340	330	477	421	370	475	381	403

All values are reported in millimeters.
[a] Includes an estimated ET = 25 mm from woodland site for DOY 1–64 when measurements were unavailable.
[b] Includes ET = 22 mm from woodland site for DOY 1–60 when measurements were unavailable.

Due to the ability of riparian plants to access groundwater, all riparian sites had annual ET in excess of precipitation (Table 2). The woodland used the greatest quantity of groundwater, ET_{gw} (Eq. (1)), but the grassland and shrubland switched ranks from year-to-year. Despite the greater depths to groundwater (Fig. 4) the two woody plant dominated sites usually had higher values of ET_{gw}. Although in 2005, the water table rose to within 1 m of the surface at the grassland (Fig. 4a) and this likely afforded the grass easier access to groundwater resulting in greater ET_{gw} than the shrubland. At about 3 m, this species of grass, *S. wrightii*, begins to lose access to groundwater (Scott et al., 2006a).

We expected a large amount of variability in ET due to the variability in *P*, but surprisingly ET_{gw} was also quite variable (Table 2). Annual groundwater use varied by as much as 73 mm at the grassland, 81 mm at the shrubland, and 42 mm at the woodland (22%, 24%, and 9%, respectively, of the lowest annual total). Woodland ET_{gw} varied the least probably due to the mature and more uniform age of the trees that result in a greater accessibility and dependency on groundwater. Though the amount of data is limited, we did not find any significant correlations of annual ET_{gw} with precipitation, growing-season precipitation, growing-season length, or potential evaporation.

4.2. Reach-level scaling

When calibrated to all of the riparian sites at one time, Eq. (2) was capable of producing very good fits to the data as characterized by the MAD and coefficient of variation (R^2; Fig. 6 and Table 3). The final form of the fitted equation is

$$ET = 11.96(1 - e^{-0.52EVI}) + 0.56\,e^{0.09T_s} - 0.87, \tag{5}$$

though there were numerous other local minima in the objective function response surface that resulted in nearly as good of fits. For validation purposes, we calibrated Eq. (2) using just 2003 data and looked at its predictions in 2004 and 2005, and we calibrated Eq. (2) using two of the sites and validated it against the remaining site (Table 3). In all cases, the model produced results that were nearly as good as or equal to the best-fit scenario.

We have evaluated the predictions of ET given by Eq. (2) at non-riparian sites and have found that the model over-predicts ET at more water-limited sites (data not shown). Therefore, determining reach-scale ET for the watershed by simply summing up the modeled ET from all the pixels within the riparian corridor would result in an over-prediction of ET as there are pixels composed entirely of, or contain significant proportions of, non-phreatophytic vegetation within the corridor (e.g., old retired agricultural fields or non-phreatophytic herbaceous vegetation). To try and account for this limitation, we used a recent high-resolution vegetation map of the riparian corridor to determine the amount (%) of riparian vegetation within each 250 m pixel in the riparian corridor. This was then multiplied by the ET predicted for that pixel before multiplying by the pixel area (250 m^2) to determine the volume of evaporated water over the year.
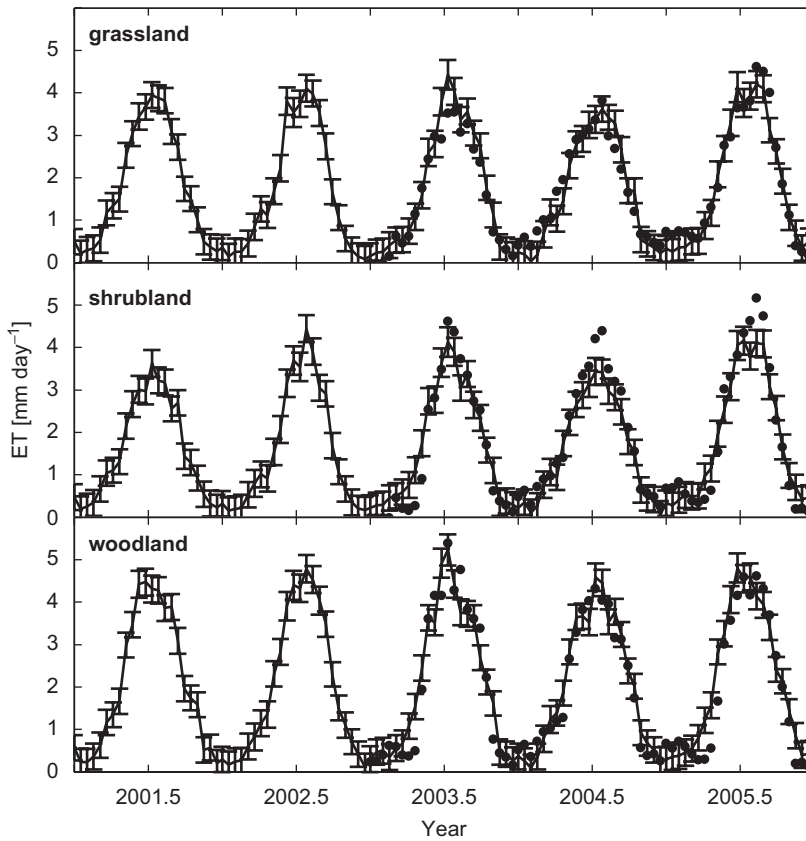
Fig. 6. Measured (solid dots) and modeled ET ($\pm\sigma_{et}$) at the three riparian sites.

Table 3
Model validation results reported as the mean absolute difference (MAD; Eq. (3)) and coefficient of determination (R^2)

Dataset used to fit equation	MAD				R^2			
	All sites	Woodland	Shrubland	Grassland	All sites	Woodland	Shrubland	Grassland
Three sites, 2003–2005 data	0.32	0.34	0.34	0.27	0.93	0.93	0.95	0.94
Three sites, 2003 only	0.35	0.33	0.40	0.33	0.93	0.94	0.95	0.95
Omitting grassland				0.29				0.94
Omitting shrubland			0.37				0.95	
Omitting woodland		0.36				0.93		

Annual reach-average ET and precipitation were not significantly correlated along the Upper San Pedro and its major tributary, the Babocomari (Table 4). While the years with the highest amount of precipitation did have higher than average ET, years with low precipitation were not always associated with below average ET. Over the 5-year period, ET was considerably less variable (coefficient of variation or CV = 0.05) than precipitation (CV = 0.13) and representative of the ability of riparian plants to buffer themselves against meteorological drought. Average annual ET on the Babocomari and San Pedro were not significantly different and reflected the phreatophytic nature of the vegetation as ET generally exceeded P by ~450 mm year^{-1} on both rivers (Table 4). The main vegetation assemblage along both rivers was dominated by mesquite (Scott et al., 2006b), the dominant tree at the woodland and shrubland sites, and average reach ET amounts are reflective of rates from these sites (Table 2).

Generally, annual riparian groundwater use along the San Pedro and Babocomari Rivers was nearly constant over the study period (Fig. 7). For the Sierra Vista Subwatershed, total riparian groundwater use ranged from $14.1–16.5 \times 10^6 \, \mathrm{m^3 \, year^{-1}}$ during the 5-year period (Table 5). For the San Pedro alone, our amounts are within the range of values reported by Scott et al. (2006b), but they are considerably greater

Table 4

Reach-average ET and precipitation (mm year^{-1}) along the Babocomari and San Pedro Rivers within the Sierra Vista Subwatershed

	Babocomari		San Pedro	
	ET	P	ET	P
2001	739	297	712	297
2002	710	215	660	216
2003	739	230	697	220
2004	673	246	660	259
2005	735	274	735	284
Mean	719	252	693	255

The computed standard errors for ET were about ±31 mm in all years.
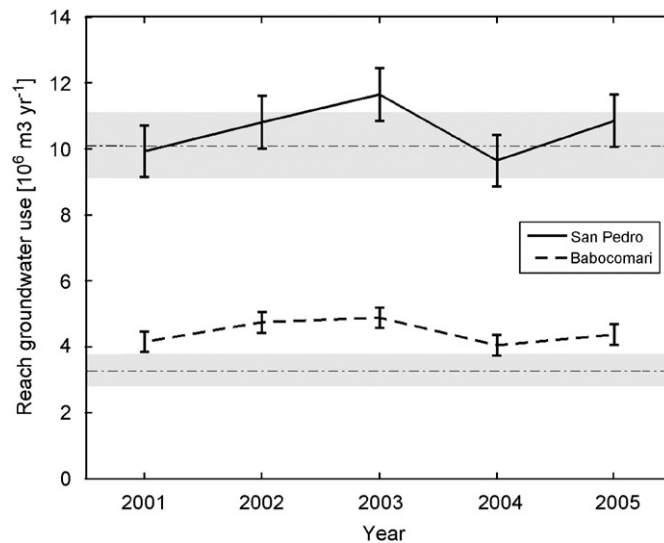
Fig. 7. 2001–2005 reach-level riparian groundwater (or ET *in excess of* precipitation) use along the San Pedro and Babocomari rivers within the Sierra Vista Subwatershed. The ranges of estimates determined by Scott et al. (2006b) for 2003 are indicated by the shaded regions.

Table 5

Annual riparian groundwater use ($\times 10^6 \, \mathrm{m^3 \, year^{-1}}$) along the Babocomari and San Pedro Rivers within the Sierra Vista Subwatershed

	Babocomari	San Pedro	Subwatershed total
2001	4.2	9.9	14.1
2002	4.7	10.8	15.5
2003	4.9	11.6	16.5
2004	4.1	9.6	13.7
2005	4.4	10.8	15.2
Mean	4.4	10.6	15.0

than the other previous estimates (Table 1). Because of our larger estimates for groundwater use for the Babocomari (by about 136%), the watershed totals (Table 5) are higher than $11.8–14.9 \times 10^6 \, \text{m}^3 \, \text{year}^{-1}$ range reported by Scott et al. (2006b) for 2003. Likewise, our estimates for the Babocomari River are about six times greater than the $0.74 \times 10^6 \, \text{m}^3 \, \text{year}^{-1}$ of Corell et al. (1996).

5. Discussion

The goal of this paper was to document 3 years of ET data collected over three riparian vegetation types and then use these data to produce multiyear estimates of riparian ET and groundwater use for the semiarid Sierra Vista Subwatershed in southern Arizona, USA. With the advent of longer term in situ ET measurements and high-frequency repeat-overpass remote-sensing data, there is a need to combine these technologies to produce hydrological products relevant to society. In order to scale up eddy covariance measurements from a variety of riparian ecosystems to estimate total watershed riparian water use over a 5-year period, we calibrated an empirical model that used data derived solely from the NASA MODIS sensor to predict well-watered riparian ET within the subwatershed. We then combined this product with spatially interpolated rainfall to estimate groundwater use by the riparian vegetation.

For the three riparian eddy covariance sites, ET always exceeded precipitation on an annual basis (Table 2). Because the dominant vegetation at the three sites was phreatophytic, they accessed groundwater throughout the growing season. Riparian ET can be viewed as a combination of a more-fixed groundwater use plus a more-variable rainfall-dependent rate. For years with greater amounts of precipitation, ET increased as evaporation was enhanced from the soil and non-phreatophytic plants. These data did not indicate to what degree the phreatophytes might switch from deeper, groundwater sources to near-surface, precipitation sources during the summer rainy season, but Potts et al. (2006) indicated that the grassland productivity is more sensitive to precipitation than the shrubland. Also, Scott et al. (2003) showed that ET of the understory of the woodland increases during the rainy season whereas the ET of the overstory was relatively constant, and gross ecosystem production (GEP) becomes more decoupled from precipitation across the grassland-to-woodland woody plant gradient (Scott et al., 2006a; Williams et al., 2006). Similarly, we found the ET_{gw} was least variable at the woodland site. With the exception of 2005 where the depth to groundwater rose to within 1 m of the surface at the grassland site (Fig. 4), groundwater use increased, despite the increasing depths to groundwater, across the grassland-to-woodland gradient. Steinwand et al. (2006) found that groundwater use decreased with depth to water and from herbaceous to woody vegetation, but the amount of phreatophyte cover also decreased substantially in their study which was not the case herein. The ratio of woodland to shrubland phreatophyte density was 1.35 (Scott et al., 2006b), but the ratio of woodland to shrubland annual groundwater use ranged from 1.1 to 1.5, indicating that these ecosystems partition their groundwater and surface water use differently.

Several methods have been proposed that use remote-sensing data to estimate ET over large areas. In general they fall into two categories: surface energy balance methods (Gillies et al., 1997) and vegetation index (VI) methods (Choudhury et al., 1994). Energy balance methods typically estimate LE by estimating the sensible heat flux using the difference between air temperature and the land surface temperature (LST), estimated by remote sensing (Moran et al., 1994). This estimate of the sensible heat flux is combined with an estimate of the available energy to estimate ET as a residual. Energy balance methods have the advantage of being physically based, so the same methods can be applied to different ecosystems and climate conditions in theory. By combining LSTs with VIs, under favorable conditions they can account for both plant transpiration and soil moisture evaporation (Carlson et al., 1995; Gillies et al., 1997). This approach requires unbiased radiometric measurement of LSTs. MODIS LSTs (1 and 5 km pixel size) or AVHRR LSTs (1 km) do not have the needed resolution for narrow riparian corridors and they capture adjacent, non-riparian land that tends to have a high surface temperature in arid and semiarid landscapes (Nagler et al., 2005a). On the other hand, finer-resolution satellite imagery, such as ETM+, does not have the needed temporal resolution to make frequent estimates of ET. Each satellite overpass produces a single, instantaneous, estimate of ET, which is subject to error due to temporal variability in energy fluxes from a vegetated surface (Kustas et al., 2002). Further research is needed to develop these methods as working tools for estimating riparian ET.

VI methods are empirical in nature, and depend on the relationship between foliage density and unstressed ET for a particular range of species and meteorological conditions. We adopted an approach that was similar to Nagler et al. (2005a, b) because the model inputs from satellite were available at the temporal (every 8–16 days over the course of 5 years) and spatial (EVI, 250 m, T_s, 1 km) resolution needed to adequately capture the seasonal to yearly dynamics of riparian ET. We calibrated our model with ET measurements from flux towers. Hence, our method used remote sensing to scale ground measurements of ET rather than to directly estimate ET by a physical model. We accept that the model should not be extrapolated to other ecosystems or climate regimes. However, such an approach when calibrated using measurements from a broader climatic region has indicated that many different riparian vegetation types have an ET that is described by the same empirical relationship (Nagler et al., 2005b). Additionally we argue that the physically based approaches that currently exist should not be applied over a region without validation using ground-based measurements as all require some level of empiricism and tuning to produce reliable estimates of ET (Kustas et al., 2007).

Our model when calibrated by using in situ ET measurements from three different riparian plant communities skillfully captured the magnitude and variability of riparian ET (Fig. 6). Likewise, using subsets of data to calibrate the model resulted in predictions for the validation datasets that were as good as the fitting Eq. (2) to all of the data (Table 3). While there are other major riparian plant communities along the San Pedro not represented in our data, our application across the entire riparian corridor was predicated on the results of Nagler et al. (2005b) who showed that ET from many different communities and even different rivers could be represented by one relationship. Further support for this was found in our validation results, which showed that one site could be accurately predicted by a calibration that used only data from the other two sites (Table 3). Because the magnitude of ET from well-watered vegetation types is primarily a function of green leaf area, fine resolution (250 m) MODIS EVI was a good indicator of this and resulted in being the primary driver of our model. Nighttime air temperature, as quantified by T_s, is primarily used as an indicator of vegetation phenology (Nagler et al., 2005a). Thus, the larger spatial resolution of T_s (1 km), which may be often capture area outside of the riparian corridor, does not hinder its use in this approach.

We estimated riparian ET for the entire Sierra Vista Subwatershed and combined these rates with interpolated annual 2001–2005 rainfall amounts from across the watershed to determine annual groundwater use. The use of a high-resolution vegetation map, along with the knowledge of what type of vegetation is phreatophytic, was necessary to screen out pixels that were primarily composed of non-riparian cover. Previous riparian groundwater use estimates for the basin have assumed all riparian vegetation of the same type (e.g., grassland, woodland, forest) within the watershed were functionally equivalent to the measurements from representative sites. Unfortunately, riparian areas are highly disturbed and comprised of patchy groupings with different vegetation ensembles (Campbell and Green, 1968) that have varying environmental drivers—all of which affects the magnitude of vegetation ET (Gazal et al., 2006). Our approach essentially accounted for variability in vegetation amount and vigor for every 250 m riparian pixel.

Stakeholders concerned about the need to supply water to the growing human population in the Sierra Vista Subwatershed and protect the base flows to the river that sustain the health of the riparian system have been developing annual aquifer water budgets since 2002. The water budgets have helped to determine how water conservation measures are working and to chart their progress towards the Congressionally mandated goal of recharge exceeding discharge from the basin by 2011. Currently, these water budgets have fixed quantities for natural recharge (from mountain front/block recharge) and natural discharge (basin subsurface and surface outflows along with riparian consumptive groundwater use). Therefore, the approach presented here can provide riparian groundwater use amounts that reflect real natural variability in phreatophyte withdrawals and improve the accuracy of a watershed's groundwater budget.

Acknowledgments

References

Bastiaanssen, W.G.M., Ahmad, M.U.D., Chemin, Y., 2002. Satellite surveillance of evaporative depletion across the Indus Basin. Water Resources Research 38, 91–99.

Bevington, P.H., Robinson, D.K., 1992. Data Reduction and Error Analysis for the Physical Sciences. McGraw-Hill, New York.

Browning-Aiken, A., Richter, H., Strain, B., Varady, R., 2004. Upper San Pedro Basin: fostering collaborative binational watershed management. International Journal of Water Resources Development 20, 353–367.

Campbell, C.J., Green, W., 1968. Perpetual succession of stream-channel vegetation in a semiarid region. Journal of Arizona Academy of Science 5, 86–98.

Carlson, T., Capehart, W., Gillies, R., 1995. A new look at the simplified method for remote-sensing of daily evapotranspiration. Remote Sensing of Environment 54, 161–167.

Choudhury, B., Ahmed, N., Idso, S., Reginato, R., Daughtry, C., 1994. Relations between evaporation coefficients and vegetation indices studied by model simulations. Remote Sensing of Environment 50, 1–17.

Cleverly, J.R., Dahm, C.N., Thibault, J.R., Gilroy, D.J., Coonrod, J.E.A., 2002. Seasonal estimates of actual evapo-transpiration from *Tamaracks ramosissima* stands using three-dimensional eddy covariance. Journal of Arid Environments 52, 181–197.

Corell, S.W., Corkhill, F., Lovvik, D., Putnam, F., 1996. A groundwater flow model of the Sierra Vista Subwatershed of the Upper San Pedro Basin—southeastern Arizona. Modeling Report No. 10, Arizona Department of Water Resources, Hydrology Division, Phoenix, AZ, 107pp.

Dahm, C., Cleverly, J., Coonrod, J., Thibault, J., McDonnell, D., Gilroy, D., 2002. Evapotranspiration at the land/water interface in a semi-arid drainage basin. Freshwater Biology 47, 831–843.

Devitt, D.A., Sala, A., Smith, S.D., Cleverly, J., Shaulis, K., Hammett, R., 1998. Bowen ratio estimates of evapotranspiration for *Tamarix ramosissima* stands on the Virgin River in southern Nevada. Water Resources Research 34, 2407–2414.

Devitt, D.A., Donovan, D.J., Katzer, T., Johnson, M., 2002. A reevaluation of the ground water budget for Las Vegas Valley, Nevada, with emphasis on ground water discharge. Journal of the American Water Resources Association 38, 1735–1751.

Falge, E., Baldocchi, D., Olson, R., et al., 2001. Gap filling strategies for long term energy flux data sets. Agricultural and Forest Meteorology 107, 71–77.

Gazal, R.M., Scott, R.L., Goodrich, D.C., Williams, D.G., 2006. Controls on transpiration in a desert riparian cottonwood forest. Agricultural and Forest Meteorology 137, 56–67.

Gillies, R., Carlson, T., Cui, J., 1997. A verification of the 'triangle' method for obtaining surface soil water content and energy fluxes from remote measurements of the Normalized Difference Vegetation Index (NDVI) and surface radiant temperature. International Journal of Remote Sensing 18, 3145–3166.

Goodrich, D.C., Scott, R., Qi, J., et al., 2000. Seasonal estimates of riparian evapotranspiration using remote and in situ measurements. Agricultural and Forest Meteorology 105, 281–309.

Huete, A., Didan, K., Miura, T., Rodreguez, E., Gao, X., Ferreira, L., 2002. Overview of the radiometric and biophysical performance of the MODIS vegetation indices. Remote Sensing Environment 83, 195–213.

Kingsolver, B., 2000. A special place—the patience of a saint: San Pedro River. National Geographic 197, 80–97.

Kustas, W., Prueger, J., Hipps, L., 2002. Impact of time averaged inputs for estimating sensible heat flux of riparian vegetation using radiometric surface temperature. Journal of Applied Meteorology 41, 319–332.

Kustas, W.P., Anderson, M.C., Norman, J.M., Li, F., 2007. Utility of radiometric–aerodynamic temperature relations for heat flux estimation. Boundary Layer Meteorology 122, 167–187.

Leenhouts, J.M., Stromberg, J.C., Scott, R.L. (Eds.), 2006. Hydrologic requirements of and consumptive ground-water use by riparian vegetation along the San Pedro River, Arizona. US Geological Survey, Scientific Investigations Report 2005-5163, 154pp.

Lines, G.C., Bilhorn, T.W., 1996. Riparian vegetation and its water use during 1995 along the Mojave River, Southern California. US Geological Survey, Water-Resources Investigations Report 96-4241.

Loheide II, S.P., Gorelick, S.M., 2005. A local-scale, high-resolution evapotranspiration mapping algorithm (ETMA) with hydroecological applications at riparian meadow restoration sites. Remote Sensing Environment 98, 182–200.

Moran, M., Clarke, T., Inoue, U., Vidal, A., 1994. Estimating crop water deficit using the relation between surface–air temperature and spectral vegetation index. Remote Sensing Environment 49, 246–263.

Nagler, P., Cleverly, J., Glenn, E., Lampkin, D., Huete, A., Wan, Z., 2005a. Predicting riparian evapotranspiration from MODIS vegetation indices and meteorological data. Remote Sensing Environment 94, 17–30.

Nagler, P.L., Scott, R.L., Westenburg, C., Cleverly, J.R., Glenn, E.P., Huete, A.R., 2005b. Evapotranspiration on western US rivers estimated using the Enhanced Vegetation Index from MODIS and data from eddy covariance and Bowen ratio flux towers. Remote Sensing Environment 97, 337–351.

Potts, D.L., Huxman, T.E., Scott, R.L., Williams, D.G., Goodrich, D.C., 2006. The sensitivity of ecosystem carbon exchange to seasonal precipitation and woody plant encroachment. Oecologia 150, 453–463.

Schaeffer, S.M., Williams, D.G., Goodrich, D.C., 2000. Transpiration of cottonwood/willow forest estimated from sap flux. Agricultural and Forest Meteorology 105, 257–270.

Scott, R.L., Shuttleworth, W.J., Goodrich, D.C., Maddock III, T., 2000. The water use of two dominant vegetation communities in a semiarid riparian ecosystem. Agricultural and Forest Meteorology 105, 241–256.

Scott, R.L., Watts, C., Garatuza, J., Edwards, E., Goodrich, D., Williams, D., Shuttleworth, W.J., 2003. The understory and overstory partitioning of energy and water fluxes in an open canopy, semiarid woodland. Agricultural and Forest Meteorology 114, 127–139.

Scott, R.L., Edwards, E.A., Shuttleworth, W.J., Huxman, T.E., Watts, C., Goodrich, D.C., 2004. Interannual and seasonal variation in fluxes of water and carbon dioxide from a riparian woodland ecosystem. Agricultural and Forest Meteorology 122, 65–84.

Scott, R.L., Huxman, T.E., Williams, D.G., Goodrich, D.C., 2006a. Ecohydrological impacts of woody plant encroachment: seasonal patterns of water and carbon dioxide exchange within a semiarid riparian environment. Global Change Biology 12, 311–324.

Scott, R.L., Goodrich, D., Levick, L., McGuire, R., Cable, W., Williams, D., Gazal, R., Yepez, E., Ellsworth, P., Huxman, T., 2006b. Determining the riparian groundwater use within the San Pedro Riparian National Conservation Area and the Sierra Vista Subwatershed, Arizona (Chapter D). In: Leenhouts, J.M., Stromberg, J.C., Scott, R.L. (Eds.), Hydrologic Requirements of and Consumptive Ground-Water Use by Riparian Vegetation Along the San Pedro River, Arizona. US Geological Survey, Scientific Investigations Report 2005-5163, pp. 107–152.

Shuttleworth, W.J., 1993. Evaporation. In: Maidment, D.R. (Ed.), Handbook of Hydrology. McGraw-Hill, Inc., pp. 4.1–4.53.

Smith, J.A., 1993. Chapter 3: Precipitation. In: Maidment, D.R. (Ed.), Handbook of Hydrology. McGraw-Hill, Inc., New York, pp. 3.1–3.47.

Steinitz, C., Arias, H., Bassett, S., Flaxman, M., Goode, M., Maddock, T., Mouat, D., Peiser, R., Shearer, A., 2003. Alternative Futures for Changing Landscapes, the Upper San Pedro Basin in Arizona and Sonora. Island Press, Washington, DC.

Steinwand, A.L., Harrington, R.F., Or, D., 2006. Water balance for Great Basin phreatophytes derived from eddy covariance, soil water, and water table measurements. Journal of Hydrology 329, 595–605.

Twine, T.E., Kustas, W.P., Norman, J.M., Cook, D.R., Houser, P.R., Meyers, T.P., Prueger, J.H., Starks, P.J., Wesely, M.L., 2000. Correcting eddy-covariance flux underestimates over a grassland. Agricultural and Forest Meteorology 103, 279–300.

Unland, H.E., Arain, A.M., Harlow, C., Houser, P.R., Garatuza-Payan, J., Scott, P., Sen, O.L., Shuttleworth, W.J., 1998. Evaporation from a riparian system in a semi-arid environment. Hydrological Processes 12, 527–542.

Westenburg, C.L., Harper, D.P., DeMeo, G.A., 2006. Evapotranspiration by phreatophytes along the lower Colorado River at Havasu National Wildlife Refuge, Arizona. US Geological Survey, Scientific Investigations Report 2006-5043, 44pp.

Williams, D.G., Scott, R.L., Huxman, T.E., Goodrich, D.C., Lin, G., 2006. Sensitivity of riparian ecosystems to moisture pulses in semiarid environments. Hydrological Processes 20, 3191–3205.

Wilson, K., Goldstein, A., Falge, E., et al., 2002. Energy balance closure at FLUXNET sites. Agricultural and Forest Meteorology 113, 223–243.

Vrugt, J.A., Gupta, H.V., Bouten, W., Sorooshian, S., 2003. A shuffled complex evolution metropolis algorithm for optimization and uncertainty assessment of hydrologic model parameters. Water Resources Research 39 (8), 1201.